

Behavior of Bridge Piles Substructure Embedded Into Soil Layers during Earthquake

Noor Ihsan Ali
Geotechnical Engineer
Civil Eng. Dep.
Al Nahrain University

Ammar A. Abdul Rahman
Civil Engineering Department
Al-Nahrain University
Ammar.arahman@yahoo.com

Abstract

The evaluation of the behavior of bridge piers with soils surrounding them during earthquakes became necessary in Iraq especially after the influential earthquakes hit middle and south of Iraq during the last few years. A three dimensional finite element model for the bridge substructure and soil surrounding the bored piles with the actual dimensions and actual properties corresponding to "Sheikh Sa'ad Bridge" in Sheikh Sa'ad district at Wasit Governorate 37km south east of Kut city is presented. The model loaded with earthquake ground motion applied as lateral forces at one side of piles cap. The Earthquake hit 11 km from Ali-Al Gharbee in Maysan Province in 2012 with a magnitude of $M_L = 4.9$ is used as the input ground motion. The response of the pier was investigated and the performance of piles and the soil surrounding them was examined. Then these typical piers and surrounding soils were checked whether they can bear the stresses induced due to these earthquake forces. From this work, it was found that typical piers used in bridges in Iraq can sustain earthquakes up to those with a magnitude of $M_L = 6.8$ maximum.

Keywords: Piers, FEA, Earthquake.

1. Introduction

The geotechnical engineers have been giving more attention to the design of foundations for earthquake resistance. A great deal of time and effort has gone into the development of better methods of analyses. This has involved a greater knowledge of earthquakes in conjunction with a better understanding of the forces they exert on foundations. New concepts have been developed concerning the earthquake resistance of foundations as determined by their ability to absorb the energy input from the earth vibration. Soil dynamics gained a considerable advancement in the last few decades. These advancements include a better understanding of the behavior of the soil subjected to dynamic loading conditions, and to the ever increasing capacity and power of electronic digital computers, which made possible vast developments and advances in numerical methods such as the finite element method.

One of the structures under detailed investigations due to seismic loads is the bridges especially their substructures and the soils surrounding them.

Earthquake damage to bridge substructures will be through many factors, such as soil conditions, excessive inertia force caused by superstructure and incorrect design of piles. According to the damage statistics of pile foundation, its failure modes are complex, but soil deformations and soil liquefaction are the most common ones.

In this research, the deformation and stresses in the soil surrounding typical piles of bridges in Iraq under actual earthquakes will be investigated.

2. Equations of Motion

The motion of the idealized substructure consisting of piles, piles cap and surrounding soil under dynamic excitation will be governed by an ordinary differential equation. The governing equation, or equation of motion, is derived for the earthquake ground motion.

2.1. Earthquake Ground Motion

No external dynamic force is applied at the level of the piles cap in the idealized substructure shown in Figure (1a). The excitation in this case is the earthquake-induced motion of the foundation, presumed to be only a horizontal component of ground motion, with displacement $u_g(t)$, velocity $\dot{u}(t)$, and acceleration $\ddot{u}(t)$. Under the influence of such an excitation, the base of the piles are displaced by an amount $u_g(t)$ if the ground is rigid, and the piles cap undergoes deformation relative to base $u(t)$. The total displacement $u^t(t)$ of the substructure is:

$$u^t(t) = u_g(t) + u(t) \quad (1)$$

From the free-body diagram of the mass shown in Figure (1b), the equation of dynamic equilibrium is:

$$F_S + F_D + F_I = F(t) \quad (2)$$

$$\{F_S\} = [K]\{u\} \quad (2a)$$

$$\{F_D\} = [C]\{\dot{u}\} \quad (2b)$$

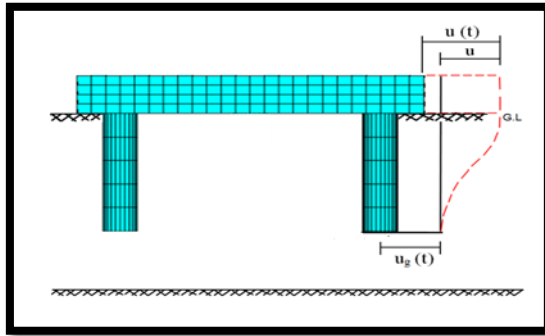
$$\{F_I\} = [m]\{\ddot{u}\} \quad (2c)$$

where:

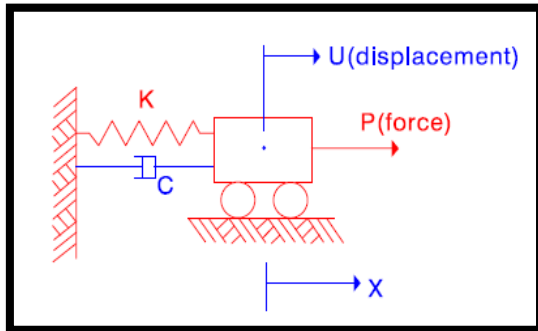
F_S : restoring force.

F_D : damping force.

F_I : inertia force.



(a)



(b)

Figure (1). Substructure idealization (a) Free body diagram (b) Bridge substructure subjected to earthquake ground motion.

Equations (2a) and (2b) still apply because the elastic and damping forces depend only on the relative displacement and velocity, not on the total quantities. However, the mass in this case undergoes acceleration u_g , and the inertia force therefore is:

$$\{F_I\} = [m]\{u''\} \quad (3)$$

This with the aid of Equation (1) can be expressed as:

$$\{F_I\} = [m]\{u''_g\} + [m]\{u''\} \quad (4)$$

Equation (2) after substitution of Equations (2a, 2b), and (4) can be expressed as:

$$[m]\{u''\} + [C]\{u'\} + [K]\{u\} = [m]\{u''_g\} \quad (5)$$

This is the equation of motion governing the deformation $u(t)$ of the idealized substructure system of Figure (1a) subjected to earthquake ground acceleration $u_g''(t)$. Comparison of Equations (2) and (5) shows that the equations of motion for the structure subjected to two excitations; the first one is the ground acceleration $= u''(t)$ and the other is the external force $-mu_g''(t)$ are one and the same. The deformation response $u(t)$ of the structure to ground acceleration will be identical to the response of the structure on fixed base due to an external force equal to mass times the ground acceleration, acting opposite to the sense of acceleration. The ground motion can therefore be replaced by an effective force $-mu_g''(t)$, [1].

3. Finite Element Analysis

In substructure analysis, the finite element method has been used as a general method of analysis when there are no other ways to formulate the differential equations governing the problem under investigation and/or no solution to the problem equations. The following basic steps are involved for any three-dimensional analysis no matter what type of element is used.

ANSYS 14.5-64bit [2] was used to model, analyze and obtain results about specimens used in this research. The description of the ANSYS logical steps for modeling and results of analysis will be explained in the following subsections.

3.1. Specimen Geometry

The finite element analysis included modeling typical bridge substructure and soil with the actual dimensions and properties corresponding to "Sheikh Sa'ad bridge" district at "Wasit" governorate 70km south of the "Kut" city in Iraq. The dimensions and properties of soil layers, bored piles and piles cap are given in tables (1), (2) and (3) respectively [3]. All lists in these tables are dynamic values which took from Geotechnical interpretive report for sheikh Saad Bridge. This bridge was carefully chosen as a typical sample for the bridges in the middle and south of Iraq for two main reasons; The first one is the availability of full record of data on soil and bridge itself (parameters required for input data for ANSYS) and the other is that its location is the nearest city point to largest earthquake in south of Iraq.

Table (1). Details about soil layers [3].

Type of soil	Depth (m)	γ_b (kN/m ³)	(E) (MPa)	Density (kg/m ³)	Dync. C_u (kN/m ²)	Dync. ϕ
Clay	14.5	20	20	1700	90	22.5
Sand	7.5	19.4	70	1700	0	40

Table (2). Details about bored piles [3].

	Diameter (m)	Depth (m)	Longitudinal Reinforcement	Stirrups
Pile	1.5	17	55 ϕ 25	ϕ 10/150 pitch

Table (3). Details about piles cap [3].

	Length (m)	width (m)	Depth (m)	Top Rein.	Bottom Rein.	Stirrups
Pile cap	12	2	1.5	9 ϕ 25 E.W.	9 ϕ 25 E.W.	ϕ 12/200

3.2. Elements Types

Using the ANSYS library of element types, the elements used in the current modeling are shown in Table (4).

Table (4). Elements used in ANSYS modeling.

ANSYS Element	Representation
SOLID45	Soil
SOLID65	Concrete
Smearred in SOLID65	Steel Reinforcement
TARGE170	Target
CONTA174	Contact

3.3. Real Constants

Data required for the calculation of the element matrices that cannot be determined from the node locations or material properties, are input as "real constants". Typical real constants include area, thickness, inner diameter, outer diameter, etc. [4].

3.4. ANSYS Modeling

The case under research was modeled using SOLID45 element which was used to model the two soil layers (clay and sand) as volumes with presence of water table at 1.5m from natural ground level. The soil model is 18m long, 9m wide and 22m deep. The distance between center to center of piles is 4.5m. The diameter of piles is 1.5m therefore distances between the centers of piles and the edges of soil volume is 5m. The distance between ends of piles and base of soil volume is 5m which is more than three times the diameter of pile because the effect of soil can be neglected beyond this distance as shown in Figure (2).

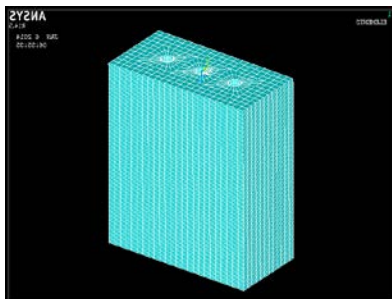


Figure 2. Soil model.

SOLID65 element, which is used for modeling three dimensional concrete with or without rebars as shown in Figure (3).

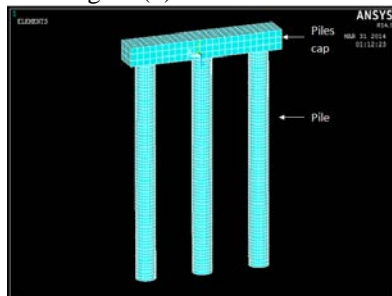


Figure 3. Pile and pile cap model.

The SOLID65 element uses a smeared rebar capability, which involves three different rebar materials orientated in any direction relative to the

global coordinate system. This smeared system was used in this research to model the reinforcement of piles. The rebar was input to replicate the volumetric ratios and orientation of the longitudinal and transverse reinforcement in the typical bridge column [5]. The material properties of the model are shown in the Table (5).

Rigid-to-flexible contact model was used to contact between the piles and the soil. In rigid-to-flexible contact problems, one or more of the contacting surfaces are treated as rigid (i.e., it has a much higher stiffness relative to the deformable body it contacts). In this research the concrete was considered the rigid material and the soil was the flexible (soft) one. A surface-to-surface contact model was used in this research. The contact elements use a "target surface" and a "contact surface" to form a contact pair. The target surface is modeled with TARGE170 element and the contact surface is modeled with CONAC174 element as shown in Figure (4) [5].

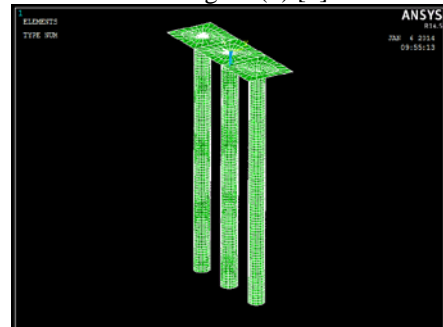


Figure (4). Contact elements around piles.

Table (5). Material properties of the model.

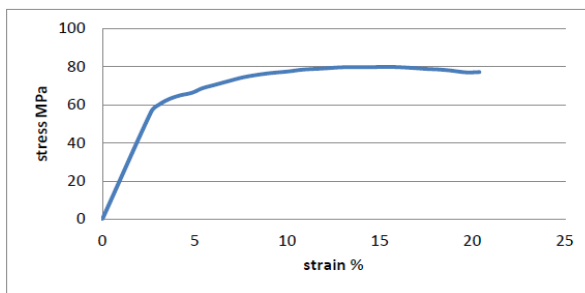
Material properties					
SOILD45	Type of soil	Ex	v	Cu kN/m ²	φ Degree
	Clay	20	0.49*	90	22.5
	Sand	70	0.33*	0	40
SOILD65	Linear Isotropic				
	EX		27229MPa **		
	DENS		2400 kg/m ³		
	NUXY		0.2		
	Multilinear Isotropic				
	Strain		Stress MPa		
	0.00036		9.8		
	0.0006		15.4		
	0.0013		27.52		
	0.0019		32.1		
	0.00243		33***		
Concrete					
Open shear crack factor			0.2		

	Close shear crack factor	0.7
	Uniaxial tensile strength	3.8 MPa
	Uniaxial compressive strength	33 MPa
Smeared Steel	Linear Isotropic	
	EX	200000 MPa
	NUXY	0.3
	Bilinear Isotropic	
	Yield Stress	414 MPa
	Tang. Mod.	20 MPa

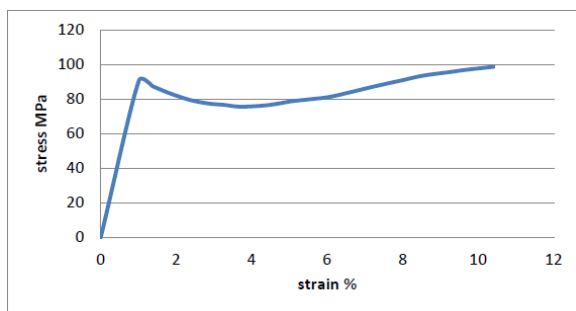
*[6], ** $E_c = 4700\sqrt{f_c'}$, *** $f_c' = 33\text{MPa}$

3.5. Non-Linear Soil Material Adopted

In order to trace the nonlinear behavior of soil, an actual stress-strain relationship for both clay and sand will be used. Figure (5a) shows the stress-strain relationship for clay with $E=20\text{MPa}$ and $c_u=90\text{ kN/m}^2$ and Figure (5b) shows the stress-strain relationship for sand with $E=70\text{MPa}$ and $\phi=40$.



(a)



(b)

Figure (5). Stress-strain relationship (a) For clay uniaxial compression [7]. (b) For sand uniaxial compression [8].

These curves were chosen because they are very close to the actual soils properties of the site under investigation

3.6. Boundary Conditions and Applied Loads

The SOLID45 element which is used to model the soil has three degrees of freedom UX, UY and UZ

per node. The main axis of pile cap is the x-axis and that along the short side of pile cap is the y-axis. Herein in this research, the earthquake loading direction will be once along the main axis of pile cap (x-axis) and then along the short side of pile cap (y-axis). To simulate the real boundary conditions for such loading:

- The base of soil volume is restrained at the bottoms in three directions.
- The sides parallel to applied earthquake loading will be restrained in perpendicular direction so when the earthquake loading will be along the main axis (x-axis) of pile cap, the boundaries of soil volume will be restrained in perpendicular direction (y-axis) and vice versa.

Two types of loads were applied to the typical model under investigation. The first load is that of the superstructure of the bridge. The superstructure load is applied as surface pressure on pile cap at the location of the three columns. The second loading is that from the earthquake ground motion are applied as lateral forces at one side of piles cap (at ground surface level) which are computed by multiplying response acceleration by the inertia mass [9]. The earthquake ground motion is considered to be applied in two perpendicular directions. The first one is when the earthquake ground motion in the same direction of the main axis of the pier (x-axis). The second loading is when the motion in the perpendicular direction to the main axis (y-axis), see Figure (6).

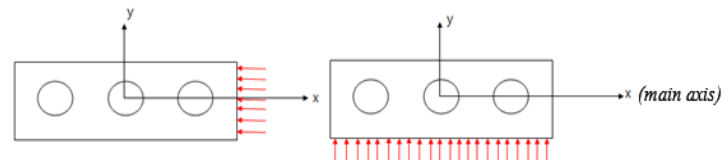


Figure (6). Earthquake ground motion direction.

Ali-Al Gharbee earthquake, happened in the south of Iraq at 15:37:02 local time on April 20, 2012 with magnitude $M_L=4.9$ with peak ground acceleration of 104.151 cm/sec^2 (0.11 g) and details shown in Figure (7) are chosen as the input ground motion for this research to give a realistic. This earthquake is chosen for the following reasons:

- 1- It is up-to-date recorded Iraqi earthquake.
- 2- To check the typical Iraqi bridge substructures to real earthquake happened in Iraq.

One cycle of earthquake motion is considered with period $T=1\text{ sec}$ and maximum amplitudes of $1.8\text{E}+6\text{ kN}$ which is the result of multiplying the PGA by the mass of the bridge substructure (175000 kg) in positive and negative directions as shown in Figure (8). Earthquake loads have been applied to the bridge substructure models in

two perpendicular directions. The first is in the x-direction which is parallel to the substructure plane and the other is in y-direction which is perpendicular to the substructure plane.

in y-direction (parallel to bridge axis) and the force act in main axis (x-direction) is much higher than that in y-direction. Therefore, the maximum displacements that occur in piles cap (at the points on which the earthquake effects were applied) approach 22.9 mm in main-direction while it approaches 31.5 mm in y-direction. Also the deformation in the top of soil in main axis (x-direction) is 13 mm while it reaches 22 mm in y-direction as shown in the Figure (9).

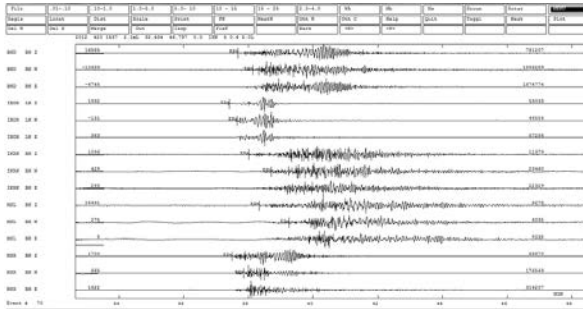


Figure (7). Ali-Al Gharbee earthquake[10]

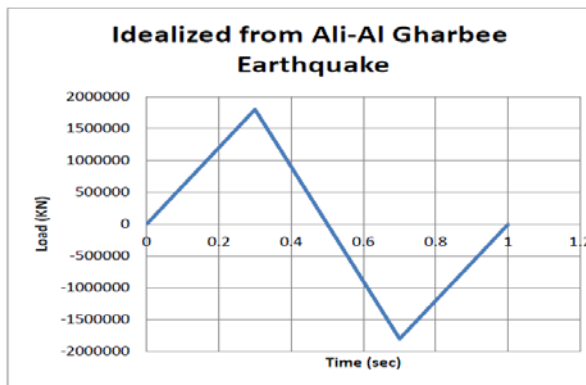


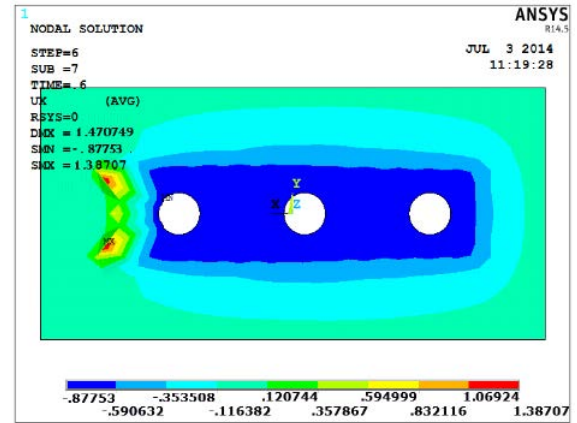
Figure (8). Earthquake's loading consider.

4. Analysis Type

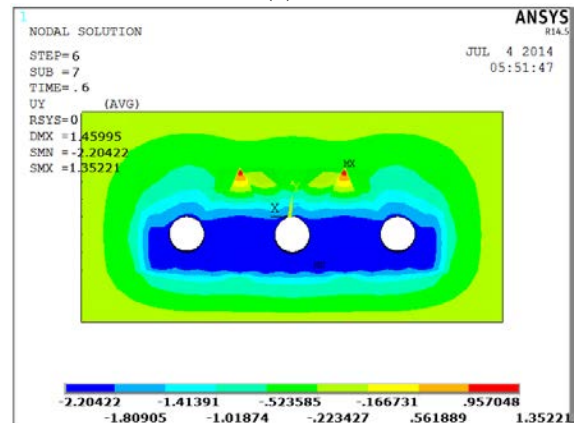
A full transient dynamic analysis will be utilized to perform a non-linear seismic analysis of soil surrounding typical pier of bridge that used in Iraq. A small displacement transient analysis was required when using SOLID45 and SOLID65 elements to gain more accurate results. Such analyses are computational expensive. However, they will give results based on the dynamic equation of equilibrium and hence both positive (tensile) and negative (compressive) stress results will be reported for the full length of the earthquake. Automatic time stepping was used and a minimum and maximum time step was specified to equal 0.0002 and 0.1 sec respectively and the load steps were ramped.

5. Analysis Results

The deformations obtained in models analyzed are due to the effects of both the super imposed dead loads and the seismic loads. The value of deformation in the models exposed to seismic loads in main axis (x-direction) is smaller than those in the models exposed to the seismic loads in perpendicular axis (y-direction). This is because the stiffness of the substructure in the x-direction (perpendicular to the bridge axis and parallel to the cross head) is much higher than that



(a)



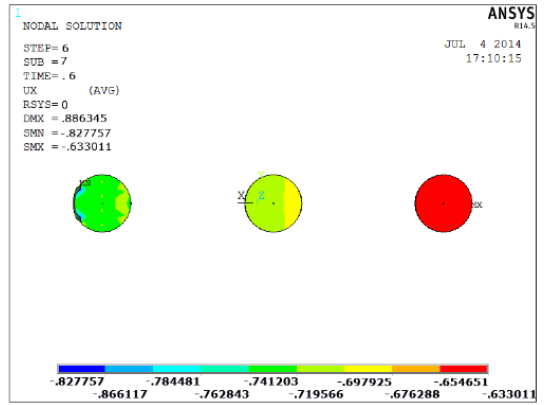
(b)

Figure (9). Deformation of soil at the top (a) In main axis direction subjected to earthquake loads in x-direction. (b) In y-direction subjected to earthquake loads in y-direction. Figure unit is (cm).

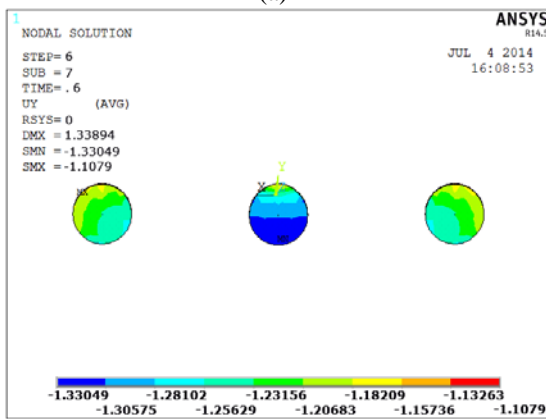
The maximum deflection occurred at the top of piles with magnitude 6 mm in x-direction when they were exposed to an earthquake load in x-direction (main axis) and -11 mm in y-direction when it was exposed to an earthquake load in y-direction (perpendicular axis to main axis) as shown in Figure (10).

The stresses calculated herein are those due to self-weight of piles and soil surrounding them plus those from the effect of earthquake ground motion plus super-structure dead loads. The maximum stress occurred at the top of clay with magnitude of 1431.094 kN/m² in x direction

subjected to earthquake loads in x-direction (main axis) and of 2750.43 kN/m² in y-direction subjected to earthquake loads in y-direction (perpendicular to main axis as shown in Figure (11). These stresses are larger than the unconfined compressive strength (q_u) for this clay obtained from the laboratory test carried out on this soil of 180 kN/m² obtained from laboratory tests carried out on this soil [3].



(a)



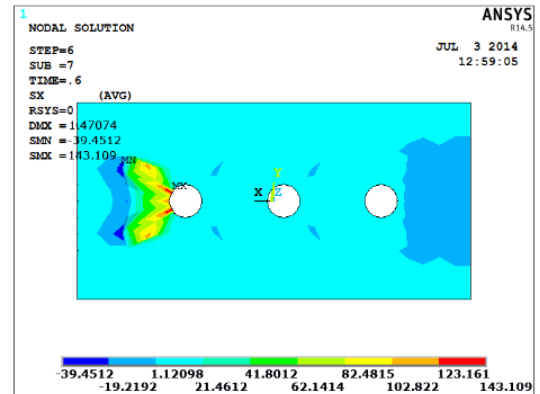
(b)

Figure (10). Deflection of piles at the (a) In x-direction (main axis) subjected to earthquake loads in x-direction. (b) In y-direction subjected to earthquake loads in y-direction at top of soil. Figure unit is (cm).

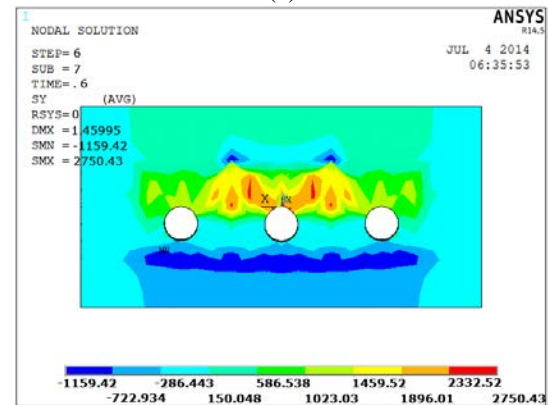
Figure (12a) show the stresses in x direction subjected to earthquake loads in x-direction (main axis). Figure (12b) show the stresses in y direction subjected to earthquake loads in y-direction (perpendicular to main axis) for soil at level 1.5 m (at water table level). Due to bearing at tip of piles the stresses occur there and those at surrounding soil become high in comparison with the stresses which occur at other layers of sand. Figure (13a) show the maximum stresses in x direction subjected to earthquake loads in x-direction (main axis). Figure (13b) show the maximum stresses in y direction subjected to earthquake loads in y-direction (perpendicular to main axis) that occur in the sand below the tip of piles.

To know how much typical piers can sustain from the earthquake ground motion, the actual Ali-AL-grabee load was increased in steps of 10% each and all element behavior were traced. It is concluded that till 1.4 of the earthquake loads, all pier elements and soil surrounding them were working normally and deformations and stresses were acceptable but when the load reached 1.5 times the earthquake load, the piles with the piles cap collapsed and solution terminated.

Accordingly, it can be concluded that typical bridge piers in Iraq can sustain earthquake loads with magnitude not more than $M_L=6.8$.

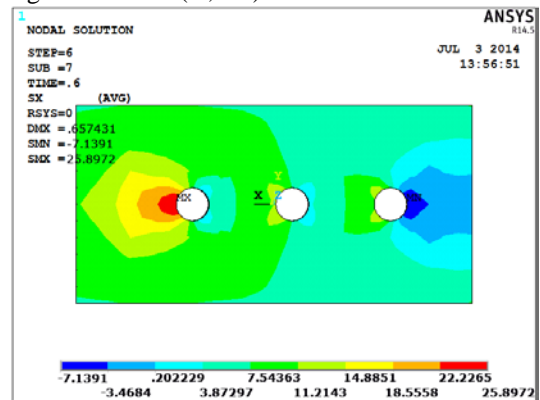


(a)

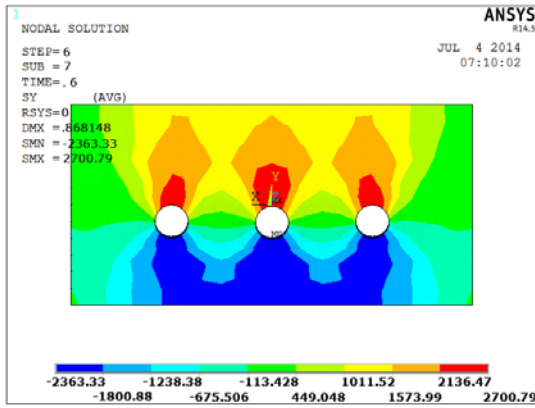


(b)

Figure (11). Stresses distribution of soil at top of clay (a) In x-direction (main axis) subjected to earthquake loads in x-direction. (b) In y-direction subjected to earthquake loads in y-direction. Figure units are (N, cm).

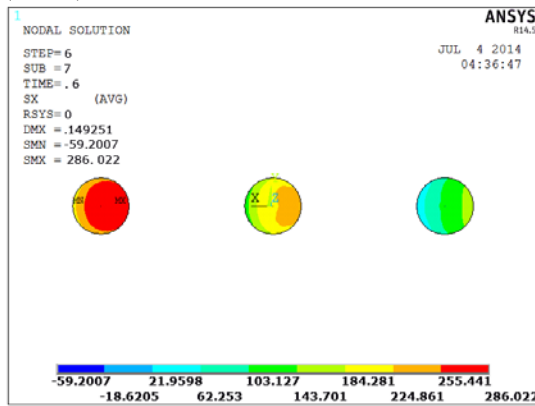


(a)

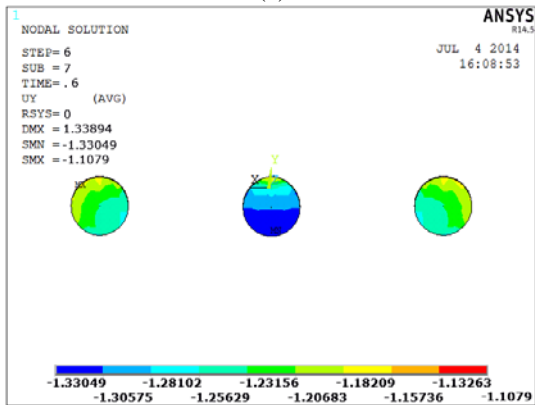


(b)

Figure (12). Stresses distribution of soil at level 1.5 m (at water table level). (a) In x-direction (main axis) subjected to earthquake loads in x-direction. (b) In y-direction subjected to earthquake loads in y-direction. Figure units are (N, cm).



(a)



(b)

Figure (13). Stresses distribution of sand under piles (a) In x-direction (main axis) subjected to earthquake loads in x-direction. (b) In y-direction subjected to earthquake loads in y-direction. Figure units are (N, cm).

6. Conclusions.

1-The stresses are high at the top of the clay layer then starts to reduce under the water table level as the presence of water inside the soil layer will work as a damping factor to the seismic

excitation. The maximum stresses in sand are under the tip of piles due to end bearing action which is more than horizontal forces action.

2-The maximum stresses in bored piles occur at the top of the piles beneath the bottom of piles cap. These stresses indicate that the piles experienced significant cracking and crushing when they were subjected to earthquake loading.

3-It can be concluded that typical bridge piers in Iraq made of bored piles and a pile cap can sustain earthquake loads with magnitude not more than $M_L=6.8$ the forces exerted from acceleration of such earthquake magnitude, will be large enough to cause severe cracking in piles. Even in magnitudes less than this value, crushing in concrete and separation in soil against piles will take place at the upper parts of the piles beneath the piles cap. This state must be considered carefully in the design.

4-Deformations induced under such magnitudes of earthquakes were small and within the limits of piles design codes of practice. The main failure if occurs was due to high stresses in piles concrete and soils surrounding them.

References

- [1] Datta T. K. (2010), "Seismic Analysis of Structures", Indian Institute of Technology Delhi, India, pp. 282.
- [2] ANSYS, "ANSYS Help", Release 14.5, Copyright 2013.
- [3] Report (2005), Geotechnical Interpretive report for Sheikh Saad Bridge, Geotechnical Labs, Dar Al-Handasah, Cairo.
- [4] Phillips, D. V., and Zienkiewics, O. C. (1976), "Finite Element Nonlinear Analysis of Concrete Structures", Journal of Structural Division, ASCE Proceedings, Part 2, Vol. 61, pp. 59-88.
- [5] Dhakal, S. (2004), "Empirical Relations for Earthquake Response of Slopes", International institute for geo-information science and earth observation Enschede, The Netherlands.
- [6] Bowles, J. E. (1988), "Foundation Analysis and Design", 5th Edition, McGraw-Hill, New York.
- [7] AL-Kubaisy B. H. (2013), "effect of silica-fume on the strength and swelling of expansive soil", M.Sc. Thesis submitted to the College of Engineering at the University of Al-Nahrain.
- [8] Head, K.H. (1982), "Manual of Soil Laboratory Testing", Pentech Press Limited, Vol. 2, land on, UK.
- [9] Wilson, E. L., Der Kiereghian, A. and Bayo, E. (1981), "A Replacement for the SRSS Method in Seismic Analysis," Earthquake and Structural Dynamics, University of Berkeley, California, Vol. 9, No. 2, 187 pp.
- [10] Ministry of Transportation/Iraqi Meteorological Organization and Seismology.

تصرف ركائز دعامات الجسور المغروسة في طبقات التربة تحت الهزات الارضية

د. عمار عبد الجبار عبد الرحمن
قسم الهندسة المدنية
جامعة النهرين

نور أحسان علي
قسم الهندسة المدنية
جامعة النهرين

الخلاصة

لقد أصبح ضروريا تقييم ركائز دعامات الجسور والتربة المحيطة بها تحت تأثير الهزات الارضية في العراق خصوصا بعد سلسلة الهزات التي ضربت جنوب العراق في الاعوام القليلة الماضية. تم نمذجة موديل ثلاثي الابعاد باستعمال العناصر المحددة والذي يحاكي ركائز دعامات والتربة المحيطة بها لجسر شيخ سعد في ناحية شيخ سعد في محافظة واسط / العراق. ثم تم تسليط الهزة الارضية التي وقعت في منطقة علي الغربي في محافظة ميسان ذات قوة $M_L = 4.9$ على هذه الركائز كونها أعلى هزة ضربت جنوب العراق مسجلة بشكل كامل وتم دراسة تصرف الركائز وحساب الاجهادات المتولدة في الركائز وطبقات التربة المحيطة بها وحساب أراحاتها مع وجود تأثير المياه الجوفية وبدونها. ثم تم تدقيق قابلية تحمل هذه الركائز لمثل هكذا هزة وتبين ان دعامات الجسور تتحمل هزات بمثل هكذا مدى وبامكانها ان تتحمل هزات ذات قوة لحد هزة بقوة $M_L = 6.8$ بدون فشل وهذا ما أوصى به هذا البحث.